

# A Chemical Genomic Analysis of Decoquinatate, a *Plasmodium falciparum* Cytochrome *b* Inhibitor

Tae-gyu Nam,<sup>†,‡,#</sup> Case W. McNamara,<sup>§,#</sup> Selina Bopp,<sup>‡</sup> Neekesh V. Dharia,<sup>‡</sup> Stephan Meister,<sup>‡</sup> Ghislain M. C. Bonamy,<sup>§</sup> David M. Plouffe,<sup>§</sup> Nobutaka Kato,<sup>§</sup> Susan McCormack,<sup>§</sup> Badry Bursulaya,<sup>§</sup> Hangjun Ke,<sup>||</sup> Akhil B. Vaidya,<sup>||</sup> Peter G. Schultz,<sup>\*,§,†</sup> and Elizabeth A. Winzeler<sup>\*,§,‡</sup>

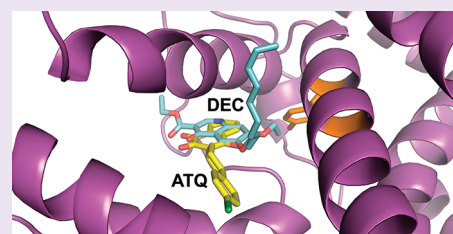
<sup>†</sup>Department of Chemistry and <sup>‡</sup>Department of Genetics, SP40-270, The Scripps Research Institute, 10550 North Torrey Pines Road, La Jolla, California 92037, United States

<sup>§</sup>Genomics Institute of the Novartis Research Foundation, 10675 John Jay Hopkins Drive, San Diego, California 92121, United States

<sup>||</sup>Center for Molecular Parasitology, Department of Microbiology and Immunology, Drexel University College of Medicine, Philadelphia, Pennsylvania 19129, United States

## S Supporting Information

**ABSTRACT:** Decoquinatate has single-digit nanomolar activity against *in vitro* blood stage *Plasmodium falciparum* parasites, the causative agent of human malaria. *In vitro* evolution of decoquinatate-resistant parasites and subsequent comparative genomic analysis to the drug-sensitive parental strain revealed resistance was conferred by two nonsynonymous single nucleotide polymorphisms in the gene encoding cytochrome *b*. The resultant amino acid mutations, A122T and Y126C, reside within helix C in the ubiquinol-binding pocket of cytochrome *b*, an essential subunit of the cytochrome *bc*<sub>1</sub> complex. As with other cytochrome *bc*<sub>1</sub> inhibitors, such as atovaquone, decoquinatate has low nanomolar activity against *in vitro* liver stage *P. yoelii* and provides partial prophylaxis protection when administered to infected mice at 50 mg kg<sup>-1</sup>. In addition, transgenic parasites expressing yeast dihydroorotate dehydrogenase are >200-fold less sensitive to decoquinatate, which provides additional evidence that this drug inhibits the parasite's mitochondrial electron transport chain. Importantly, decoquinatate exhibits limited cross-resistance to a panel of atovaquone-resistant parasites evolved to harbor various mutations in cytochrome *b*. The basis for this difference was revealed by molecular docking studies, in which both of these inhibitors were shown to have distinctly different modes of binding within the ubiquinol-binding site of cytochrome *b*.



Malaria remains one of the most devastating infectious diseases in the world. More than 750,000 deaths from malaria were reported in 2009 with a significant portion of the victims being children under the age of five.<sup>1</sup> The absence of a viable vaccine places additional importance on chemotherapy to control malaria and treat infected individuals. Although many useful antimalarial drugs have been developed, continued emergence and dissemination of drug-resistant parasites have compromised the efficacy of many of the available malaria treatments (reviewed in ref 2). This list includes 4-aminoquinolines, antifolate inhibitors, and atovaquone, an analogue of ubiquinone. The latter is a cytochrome *bc*<sub>1</sub> complex inhibitor and a leading antimalarial used in treatment and causal prophylaxis.

A traditional approach to antimalarial drug discovery has been to identify high-value targets, purify recombinant protein, and then perform biochemical assays to identify inhibitors (reviewed in ref 3). Alternatively, *in silico* approaches in which compounds are docked to the structures of predicted targets have also been used in lieu of biochemical screening to generate rationale drug discovery leads.<sup>4,5</sup> A shortcoming of target-based approaches is that identified targets may not be essential. For example, the FabI enzyme was originally thought to be a high-quality target, but recent experiments have shown the FAS-II pathway to be nonessential for parasite blood stages.<sup>6</sup> Furthermore, inhibition of the purified target may not

necessarily translate to the parasite due to competing physiological and metabolic factors that may be difficult to predict or reproduce. Therefore, a better approach might be to select targets that have been chemically validated in cell-based assays and to perform secondary biochemical screens on these targets.

To identify chemically validated targets, we performed a high-throughput screen against an annotated compound library of 28,000 known drugs and natural products preselected to have drug-like characteristics. Decoquinatate, a compound currently used as a coccidiostat, showed the greatest selectivity for *Plasmodium falciparum*, reflected by the high therapeutic index, and was selected for further chemical genetic analysis and target discovery. We show here using genetic, biological, and *in silico* approaches that decoquinatate targets the ubiquinol-binding pocket of *P. falciparum* cytochrome *b* (*Pf*CYT*b*).

## RESULTS AND DISCUSSION

**Screening an Annotated Compound Library To Discover Antimalarials.** Our initial goal was to identify antimalarial

**Received:** April 1, 2011

**Accepted:** August 25, 2011

**Published:** August 25, 2011

Table 1. Therapeutic Index of Selected Screen Hits from the Annotated Compound Library

compound	mode of action	<i>P. falciparum</i> <sup>a</sup> IC <sub>50</sub> (nM) <sup>c</sup>	mammalian cell line <sup>b</sup> CC <sub>50</sub> (μM) <sup>d</sup>	therapeutic index CC <sub>50</sub> /IC <sub>50</sub>
Gramicidin A	antibiotic	2	0.11	55.0
Muconomycin B	antibiotic	2.4	0.03	12.5
Verrucarin J	antibiotic	2.4	0.029	12.1
<b>Decoquinat</b>	<b>anticooidal</b>	<b>4.3</b>	<b>&gt;12.5</b>	<b>&gt;2,500</b>
Valinomycin	antibiotic	7.1	0.091	12.8
Ciproquinat	anticooidal	8	>1.25	>156
<b>F-HHSiD</b>	<b>antiemetic</b>	<b>16</b>	<b>9.77</b>	<b>610.6</b>
Anisomycin	protein synthesis inhibitor	20	ND <sup>e</sup>	
Synthalin	antidiabetic	27	>5.4	>200
Prodeconium	neuromuscular inhibitor	40	>6.25	>156
<b>YM-95831</b>	<b>antihyperlipidemia</b>	<b>48</b>	<b>&gt;12.5</b>	<b>&gt;260</b>
Edatrexate	antitumor	69	0.005	0.1
HHSiD	antiemetic	76	>1.25	>16.4
Borrelidin	antiviral	83	0.959	11.6
Carbostyryl 127	antihistamine	85	ND	
Puromycin	antineoplastic	88	>1.25	>14.2
Aurantimycin A	antibiotic	92	0.045	0.5
Tracazolate	GABA agonist	120	ND	
Lasalocid A	antibiotic	200	ND	
Strobilurin B	cytochrome <i>bc</i> <sub>1</sub> inhibitor	230	3.1	13.5
SKF-105685	anti-inflammatory	300	ND	
Gentian violet	antifungal	319	>1.25	>4
Demecarium	cholinergic	380	ND	
Berberine	antiprotozoan	500	0.32	0.6
NSC 57153	antitumor	500	0.55	1.1
Clofilium	hERG channel blocker	524	>1.25	>2.4
Tilorone	antiviral	1000	>12.5	>12.5
Sulotidil	vasodilator	1700	0.97	0.6
Bufexamac	anti-inflammatory	3000	ND	
Verapamil	antihypertensive	3800	ND	

<sup>a</sup> *P. falciparum* 3D7 strain. <sup>b</sup> Murine pro-B cell line Ba/F3. <sup>c</sup> IC<sub>50</sub> 50% inhibitory concentration measured by 72 h-SYBR Green parasite proliferation assay

<sup>d</sup> CC<sub>50</sub> 50% cytotoxicity concentration measured by CellTiter Glo reagent <sup>e</sup> ND = not determined.

compounds that could be used in subsequent target identification studies. The screen hits from a previous high throughput, cell-based screen of blood stage *P. falciparum* carried out with an annotated compound library (>28,000 compounds) were evaluated.<sup>7</sup> In contrast to random small molecule libraries used in other high-throughput screens,<sup>7–10</sup> these compounds have drug-like characteristics and have the advantage of being available from vendors, eliminating the need for chemical resynthesis. The initial screen detected 104 compounds (~0.4% hit rate) that inhibited parasite proliferation by 50% at concentrations less than 1.25 μM. On the basis of compound availability and the presence of a unique chemical scaffold, 30 of the 104 compounds were subsequently selected and retested in a dose-response assay (Table 1).

Compounds with antimalarial activity were next evaluated for parasite selectivity by comparing the ratio of the 50% inhibitory concentration (IC<sub>50</sub>) value measured against *P. falciparum* 3D7 strain and the 50% cytotoxicity concentration (CC<sub>50</sub>) measured against Ba/F3 cells, an immortalized murine bone marrow-derived pro-B-cell line. The resultant therapeutic index (CC<sub>50</sub>/IC<sub>50</sub>) is a good indicator of compound selectivity and showed YM-95831 (>260), F-HHSiD (610), and decoquinat (>2,500) to have the greatest ratios (Table 1). The high selectivity of these compounds

combined with scaffolds unique among known antimalarials (Figure 1) made these interesting candidates for further investigation (extended discussion in Supporting Information).

To further prioritize these compounds, we examined their pharmacokinetic properties. While YM-95831 retained high selectivity *in vitro* between panels of drug-resistant parasites (Supplementary Table 1) and mammalian cell lines (Supplementary Table 2), it showed extremely low plasma exposure (*t*<sub>1/2</sub> < 30 min; Supplementary Table 3) when administered orally to mice. Likewise, F-HHSiD was also eliminated from the mouse bloodstream so rapidly (*t*<sub>1/2</sub> < 30 min; Supplementary Table 3) that it was below detectable limits in the plasma less than 30 min after oral administration. Decoquinat, on the other hand, has been reported to have excellent pharmacokinetic properties (*t*<sub>1/2</sub> = 9–22 h (iv) in chickens<sup>11</sup>). This may be due to the long lipophilic side chain at the R<sup>1</sup> position because ciproquinat (Figure 1, panel a), a short chain derivative of decoquinat, has potent antimalarial activity in our assay (IC<sub>50</sub> = 5 nM; Table 1) but suffers from poor oral pharmacokinetics (*t*<sub>1/2</sub> < 30 min; Supplementary Table 3). Taken together, not only does decoquinat have an attractive chemical scaffold,<sup>12</sup> but it also has an optimized side chain for an improved pharmacokinetic profile. As a result of these characteristics, we selected decoquinat for target identification studies.

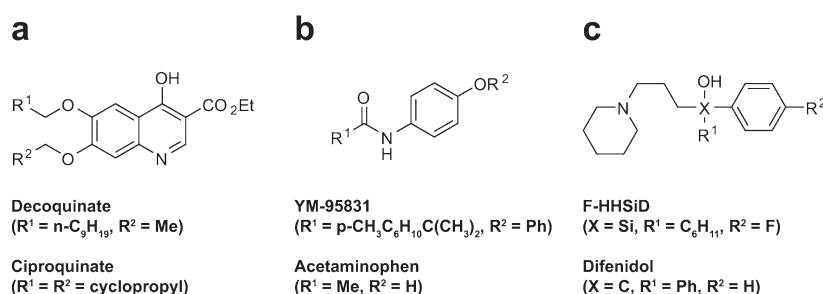


**Figure 1.** Chemical structures of (a) decoquinates, (b) YM-95831, and (c) F-HHSiD. Relevant analogues are included for each.

**Genome Scanning of a Decoquinates-Resistant Line Reveals Mutations in Cytochrome *b*.** To elucidate the biological target(s) of decoquinates, we combined *in vitro* selection of decoquinates-resistant (DEC-R) parasites<sup>13,14</sup> with genome scanning.<sup>15</sup> It has been shown that *P. falciparum* often acquires genomic changes in the gene encoding the drug target in response to selection pressure. These changes can be readily detected on a high-density DNA microarray or, alternatively, by whole genome sequencing. Selection of UV-irradiated parasites with increasing concentrations of decoquinates leads to the emergence of DEC-R parasites (Supplementary Figure 1, panel a). A clonal line of DEC-R parasites was subcloned from the resistant culture for analysis by DNA microarray and dose-response analysis confirmed a 90-fold increase in the  $\text{IC}_{50}$  compared to the decoquinates-sensitive parental strain (Supplementary Figure 1, panel b).

The array has been previously used to detect both newly acquired single nucleotide polymorphisms (SNPs) and copy number variations (CNVs).<sup>15–18</sup> Genome scanning revealed that the DEC-R clone did not acquire CNVs in the nuclear genome (Supplementary Table 4); however, potential coding mutations were detected in three genes ( $P$ -value cutoff of  $1 \times 10^{-10}$ ). A less stringent cutoff of  $1 \times 10^{-5}$  identified potential SNPs in 13 additional genes (Supplementary Table 5), including dihydroorotate dehydrogenase (*pfhdod*; PFF0160c) whose gene product interacts with *PfCYTb* and could represent an important second site mutation. Sequencing of *PfDHOD* showed that this potential lesion was a false positive, which is consistent with the high  $P$ -value assigned to this prediction. Manual inspection of the microarray data for the other 12 genes supported that these genes were also false positives. The three genes with the greatest probability of containing a SNP were genes encoding a hypothetical protein on chromosome 14 (PF14\_0110), protein kinase 4 (PFF1370w), and the mitochondrially encoded *PfCYTb* (*mal\_mito\_3*; *pfcytb*; Supplementary Table 5). The strongest signal from this group of genes was from that detected in *pfcytb* (Figure 2, panel a; false positive probability =  $1 \times 10^{-72}$ ). Direct sequencing of *pfcytb* validated the array signal and revealed two closely spaced, nonsynonymous SNPs resulting in A122T and Y126C amino acid mutations. Although the SNPs in both PFF1370w and PF10\_0110 could be important, the SNP in *pfcytb* was considered the most promising.

*PfCYTb* is a critical subunit in the cytochrome *bc*<sub>1</sub> complex. Located in the inner mitochondrial membrane, the cytochrome *bc*<sub>1</sub> complex is an essential component of the electron transport chain (ETC) and is responsible for pyrimidine biosynthesis. The ability of decoquinates to inhibit electron transport in *Eimeria* spp.<sup>19</sup> is consistent with decoquinates targeting *PfCYTb*. Furthermore, studies of *in vitro*-derived decoquinates resistance in *Toxoplasma gondii* revealed that mutations in cytochrome *b* diminished decoquinates potency.<sup>20</sup> Importantly, *PfCYTb* has also been

identified as the target of atovaquone,<sup>21–24</sup> a clinically licensed antimalarial drug currently used in combination therapies, including Malarone. Interestingly, the DEC-R clone exhibited limited cross-resistance to atovaquone with a 4-fold loss of atovaquone potency (Figure 2, panel b). This suggests that atovaquone and decoquinates have a shared mode of action/resistance.

**Decoquinates Exhibits *in Vitro* and *in Vivo* Liver Stage Activity.** Allelic exchange cannot be performed on the mitochondrial genome, so we sought alternative methods to validate that the *PfCYTb* mutations of the DEC-R line confer decoquinates resistance. First, we hypothesized that if cytochrome *bc*<sub>1</sub> complex were the target, decoquinates, like atovaquone, would be active in hepatic stages of the parasite.<sup>25</sup> Sporozoites were assayed for their ability to develop within human hepatocytes expressing murine CD81, an essential surface protein required by the parasite for successful invasion.<sup>26,27</sup> As expected, atovaquone showed low nanomolar liver stage activity (1.70 nM) that was comparable to the  $\text{IC}_{50}$  value observed against blood stage parasites. Impressively, decoquinates showed a 10-fold increase in activity over atovaquone with an  $\text{IC}_{50}$  value of 177 pM (Figure 2, panel c) supporting the hypothesis that decoquinates shares properties with atovaquone, including inhibition of the cytochrome *bc*<sub>1</sub> complex. In contrast, the DMSO control had no effect on parasite or hepatocyte proliferation. To confirm these results, decoquinates was used in an animal prophylaxis test in which mice are given a single 50 mg  $\text{kg}^{-1}$  oral dose at the same time as receiving 50,000 *P. yoelii* sporozoites injected intravenously. Four of five mice treated with decoquinates survived, whereas one developed delayed patent parasitemia on day 7 (Table 2). All five untreated mice developed patent parasitemia within 3 days and needed to be euthanized at day 7, whereas those five given a single 2.5 mg  $\text{kg}^{-1}$  dose of atovaquone were completely protected and survived.

**Decoquinates Inhibits the Electron Transport Chain in *Plasmodium falciparum*.** To obtain further support that decoquinates works by inhibiting the electron transport chain, we used transgenic parasites in which the cytochrome *bc*<sub>1</sub> complex is rendered nonessential. *P. falciparum* parasites rely exclusively on a type 2 dihydroorotate dehydrogenase (*PfDHOD*) to synthesize orotate, a precursor for pyrimidine biosynthesis, from dihydroorotate.<sup>28</sup> Flavinmononucleotide (FMN), an essential cofactor of *PfDHOD*, mediates an intermolecular electron transfer in which the hydride equivalent from the dihydroorotate is transferred to ubiquinone ( $\text{CoQ}_{10}$ ) and creates dihydroubiquinone ( $\text{CoQH}_2$ ).<sup>29</sup> Thus,  $\text{CoQ}_{10}$  functions as the final electron acceptor in dihydroorotate oxidation, and the cytochrome *bc*<sub>1</sub> complex is required to reoxidize  $\text{CoQH}_2$  to  $\text{CoQ}_{10}$ .<sup>24</sup> On the other hand, *Saccharomyces cerevisiae* encodes a type 1A DHOD (*SdDHOD*), which performs the same conversion of dihydroorotate to orotate<sup>30</sup> but utilizes fumarate as the final electron



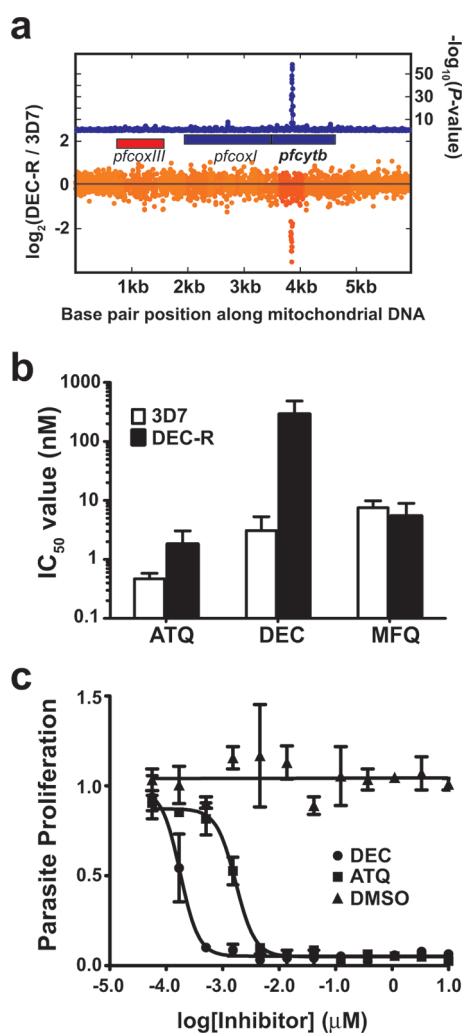


**Figure 2.** Decoquinat has a resistance and activity profile similar to that of atovaquone. (a) The  $-\log(P\text{-value})$  for hybridization differences ( $z$ -test; blue line) is shown for *pfcytb* and flanking DNA. The spike is characteristic of a detected SNP. Below the gene model, the loss of hybridization resulting from the polymorphism was visualized probe-by-probe by plotting the  $\log_2$  ratio of probe intensities in the decoquinat-resistant line versus the parental 3D7 line. (b) The  $IC_{50}$  values for atovaquone (ATQ), decoquinat (DEC), and mefloquine (MFQ) are shown for the parental 3D7 strain (white bars) and the DEC-R line (black bars). Statistically significant differences between  $IC_{50}$  values of the parental 3D7 line and the DEC-R line were calculated by a two-tailed unpaired  $t$  test:  $*P < 0.001$ . (c) Inhibition curves of decoquinat (circles) and atovaquone (squares) against *P. yoelii* sporozoites in human liver cells. The  $IC_{50}$  values were calculated using a nonlinear regression curve fit. Atovaquone was determined to have an  $IC_{50}$  value of 1.7 nM, whereas decoquinat had activity equivalent to that of atovaquone at one log lower inhibitor concentration ( $IC_{50} = 177$  pM). DMSO had no effect on the culture.  $IC_{50}$  values for all experiments are represented as means  $\pm$  SD and were calculated from at least two independent experiments performed in duplicate.

acceptor instead of  $CoQ_{10}$ . As a result, the enzymatic activity of ScDHOD functions independently of the cytochrome  $bc_1$  complex, rendering it nonessential in transgenic parasites expressing ScDHOD in the D10 strain (ScDHOD-D10). Therefore, cytochrome  $bc_1$  inhibitors are expected to show a significant loss of potency against the ScDHOD-D10 line relative to the parental D10 line.<sup>22</sup>

In this study, we utilized ScDHOD-D10attB parasites in which a single copy of the ScDHOD gene was integrated (see Methods). Atovaquone, a validated inhibitor of the cytochrome  $bc_1$  complex, as expected showed a large shift in its  $IC_{50}$  value ( $>1900$ -fold shift) against the ScDHOD-D10attB line (Table 3). A  $>180$ -fold shift in the  $IC_{50}$  of decoquinat was observed in the ScDHOD-D10attB line (Table 3) indicating that the primary mode of action for decoquinat is inhibition of the mitochondrial ETC. Predictably, no shift was observed for anisomycin, an antimalarial that inhibits protein synthesis. However, the transgenic parasite line demonstrated a slight increase in mefloquine sensitivity (Table 3).

To confirm the results from the transgenic strain, mitochondrial membranes were prepared from *P. yoelii* and cytochrome  $c$  reductase activity was assayed with atovaquone and decoquinat (Supplementary Figure 2). An  $IC_{50}$  value of 7.6 nM was calculated for atovaquone and 97 nM for decoquinat. Both values are comparable to the cell-based activity determined from the SYBR Green-based proliferation assay. These data further support that the primary mode of action of decoquinat is to inhibit the cytochrome  $bc_1$  complex.

**Molecular Modeling of Two Different Inhibitor Classes to Cytochrome  $b$ .** We next performed molecular modeling to elucidate the underlying molecular mechanism for limited cross-resistance between atovaquone and decoquinat. *PfCYTb*, the putative target of each inhibitor, is a catalytically important subunit of the cytochrome  $bc_1$  complex. Two discrete reaction sites,  $Q_o$  and  $Q_i$ , have been characterized within *PfCYTb*.  $Q_i$  is the ubiquinone reduction site, and  $Q_o$  is the ubiquinol oxidation site. Both sites are druggable, and inhibitors have been classified by which binding pocket they target.  $Q_o$  site binders are known as class I inhibitors, whereas  $Q_i$  site binders are called class II inhibitors.<sup>31</sup> Previous investigations have delineated that two general modes of binding persist for class I inhibitors.<sup>32,33</sup> Class Ia inhibitors of  $Q_o$  typically contain a  $\beta$ -methoxyacrylate (MOA) substituent exemplified by MOA-stilbene (MOAS); however, non-MOA-containing inhibitors, such as famoxadone, are also representative of this subclass (Figure 3, panel a). Class Ib inhibitors of  $Q_o$  include stigmatellin A and atovaquone (Figure 3, panel a) and often possess a chromone ring. This class of inhibitors is further characterized by their interaction with a histidine residue from the neighboring Rieske iron–sulfur protein (ISP) comprised within the cytochrome  $bc_1$  complex.

Decoquinat has a chemical scaffold similar to those of some of the  $Q_o$  inhibitors but does not match to either subclassification. Therefore, we initiated molecular dynamics and energy minimization studies of decoquinat with a homology model of *PfCYTb* to help resolve the most likely mode of binding. The results of the docking studies support that decoquinat belongs to class Ia inhibitors. Superposition of the energy minimized structure of decoquinat overlays more closely with the positioning of famoxadone and MOAS in co-crystallographic studies<sup>34</sup> (Figure 3, panel b). Importantly, the ethyl carboxylate substituent of decoquinat is predicted to occupy the same binding space as the MOA substituent in MOAS and the heterocyclic ring in famoxadone. This predicted mode of binding is significant because it places each of the aforementioned substituents proximal to helix C. Amino acid residues 122 and 126, the site of decoquinat-resistance mutations, both reside in this helix. Presumably the positioning of decoquinat relative to the A122T and Y126C mutations alters the structural complementarity between the  $Q_o$  pocket and decoquinat thereby reducing the binding affinity. It should be noted that Glu261 preferentially

**Table 2. Test of Decoquinatone's Ability To Provide Causal Prophylaxis from *P. yoelii* Infection**

	dose <sup>a</sup> (mg kg <sup>-1</sup> )	vehicle	animals tested	parasitemia <sup>b</sup> (%)	prepatent period <sup>c</sup> (days)
untreated	n/a		5	100	3
decoquinatone	50	corn oil	5	20	8
atovaquone	2.5	0.5% HPC <sup>d</sup> + 0.1% Tween-80	5	0	n/a

<sup>a</sup> Oral administration (po). <sup>b</sup> Parasitemia represents animals with blood stage parasites detected by microscopy. <sup>c</sup> Prepatent period represents the day at which parasitemia was first observed. <sup>d</sup> Hydroxypropyl cellulose.

**Table 3. Summary of IC<sub>50</sub> Values between a Transgenic Line Insensitive to ETC Inhibitors and the Parental Line**

<i>P. falciparum</i> strains	IC <sub>50</sub> values (nM) <sup>a</sup>			
	decoquinatone	atovaquone	anisomycin	mefloquine
D10attB	5.30 ± 1.24	0.512 ± 0.164	19.40 ± 2.07	7.88 ± 1.64
ScDHOD-D10attB	>1,000	>1,000	25.17 ± 3.76	4.02 ± 1.40

<sup>a</sup> IC<sub>50</sub> values are represented as means ± SD and were calculated from three independent experiments performed in duplicate with the SYBR Green cell proliferation assay.

adopts a rotamer that extends away from the class Ia inhibitors, whereas Glu261 in the co-crystal of stigmatellin A extends toward the inhibitor and is in hydrogen bond distance with the hydroxyl group of stigmatellin A.

Examination of the positioning of stigmatellin A in the Q<sub>6</sub> pocket from crystallographic studies<sup>33</sup> shows that class Ib inhibitors do not bind as deeply into the pocket. Instead they favor the distal region from helix C where this class can more easily interact with the histidine residue from the Rieske ISP (Figure 3, panel c). Although crystallographic data do not exist for atovaquone, an *in silico* investigation into atovaquone's mode of binding here supports that it is a class Ib inhibitor. The model by Kessl *et al.* also predicts that atovaquone forms a hydrogen bond with the histidine residue from the Rieske ISP, which is characteristic of class Ib inhibitors.<sup>35</sup> Collectively, the classification of atovaquone as a class Ib inhibitor, the distinctly different mode of binding predicted for decoquinatone, the unique decoquinatone resistance SNPs in helix C, and the limited cross-resistance with atovaquone in the DEC-R line are supportive of decoquinatone adopting a class Ia mode of inhibition.

**Decoquinatone Possesses Limited Cross-Resistance against Atovaquone-Resistant Lines.** Finally, we sought to test the modeling predictions by examining whether decoquinatone would be active against a panel of atovaquone-resistant (ATQ-R) lines with various mutations in the CoQ<sub>10</sub>-binding (Q<sub>6</sub>) site. Mutation of residue 133 from methionine to isoleucine (M133I) is a common resistance mutation observed in cultures derived from *in vitro* atovaquone selection.<sup>23</sup> The M133I mutation is present in three of five ATQ-R lines. Also a fourth line has a methionine to valine mutation at 133 that has not been described before. Both the isoleucine and valine mutations at residue 133 resulted in a ~16-fold loss in atovaquone potency (Figure 4, panel a), whereas mutation of residue 133 did not alter the IC<sub>50</sub> value of decoquinatone (Figure 4, panel b). The same was true for residue 144, which reduced atovaquone's potency by ~200-fold but had no effect on decoquinatone's potency. The triple mutant (M133I/V140T/L181V) results in a 5-fold loss in decoquinatone potency, whereas these same mutations result in a 2000-fold loss in

atovaquone potency. Finally, the single mutation of residue 267 from phenylalanine to valine (F267V) had a more moderate effect with only a 2-fold loss in decoquinatone potency while decreasing atovaquone potency by 20-fold. The control compound anisomycin had nearly invariable IC<sub>50</sub> values for the ATQ-R lines, except for a slight loss of potency *versus* the double mutant (Figure 4, panel c), whereas mefloquine was more variable and showed a 2-fold shift in multiple strains (Figure 4, panel d), suggesting that additional modifiers of drug resistance may have arisen in these strains. Finally, we could not confidently establish, one way or the other, whether a fitness cost was associated with the ATQ-R lines.

**Conclusions and Implications.** The ETC in the mitochondria represents a desirable target for antimalarials because of the parasite's reliance on this pathway in both liver and blood stages. For this reason, PfDHOD, an essential enzyme in the ETC and *de novo* pyrimidine biosynthesis, has become an attractive drug target.<sup>8</sup> Alternatively, the identification of cytochrome *bc*<sub>1</sub> inhibitors with limited or no cross-resistance to atovaquone is also a viable option.<sup>36</sup> Our experiments indicate decoquinatone and atovaquone have different and highly specific interactions within the ubiquinol-binding site of PfCYTb. The mutations conferring decoquinatone resistance have not been observed in any *P. falciparum* ATQ-R lines to date,<sup>23,37–39</sup> suggesting that these residues are more important to decoquinatone binding than atovaquone binding. Furthermore, limited cross-resistance was observed for decoquinatone against ATQ-R lines, which supports the molecular model that each of these compounds adopts a different mode of binding within the ubiquinol-binding site of PfCYTb.

Whether PfCYTb possesses the ability to simultaneously bear mutations that confer both atovaquone (*i.e.*, M133I) and decoquinatone (*i.e.*, A122T and Y126C) resistance remains to be determined. Mutations conferring atovaquone resistance in the ubiquinol-binding pocket of yeast cytochrome *b* have been linked to a fitness cost,<sup>40</sup> which suggests dual resistance to class Ia and Ib inhibitors may be challenging for the parasite. Likewise, Japrun *et al.* observed that the combination of two drug classes (pyrimethamine and WR99210) that have different modes of binding to the folate pocket of *P. falciparum* dihydrofolate reductase helped to curtail the rapid acquisition of resistance mutations.<sup>41</sup> It would thus be worth examining whether the combined use of class Ia and Ib inhibitors of cytochrome *b* would yield similar *in vitro* success.

Nevertheless, the development of next-generation cytochrome *bc*<sub>1</sub> inhibitors as antimalarials has been plagued by poor species selectivity, limited compound solubility, and low metabolic stability.<sup>36</sup> A recent medicinal chemistry effort demonstrated that 4-quinolone analogues with improved physicochemical properties could be achieved without sacrificing *in vitro* antimalarial activity and maintaining little to no cross-resistance with atovaquone.<sup>42,43</sup> While promising, decoquinatone requires further investigation to determine if it is a suitable starting point for a next-generation cytochrome *bc*<sub>1</sub> complex inhibitor.

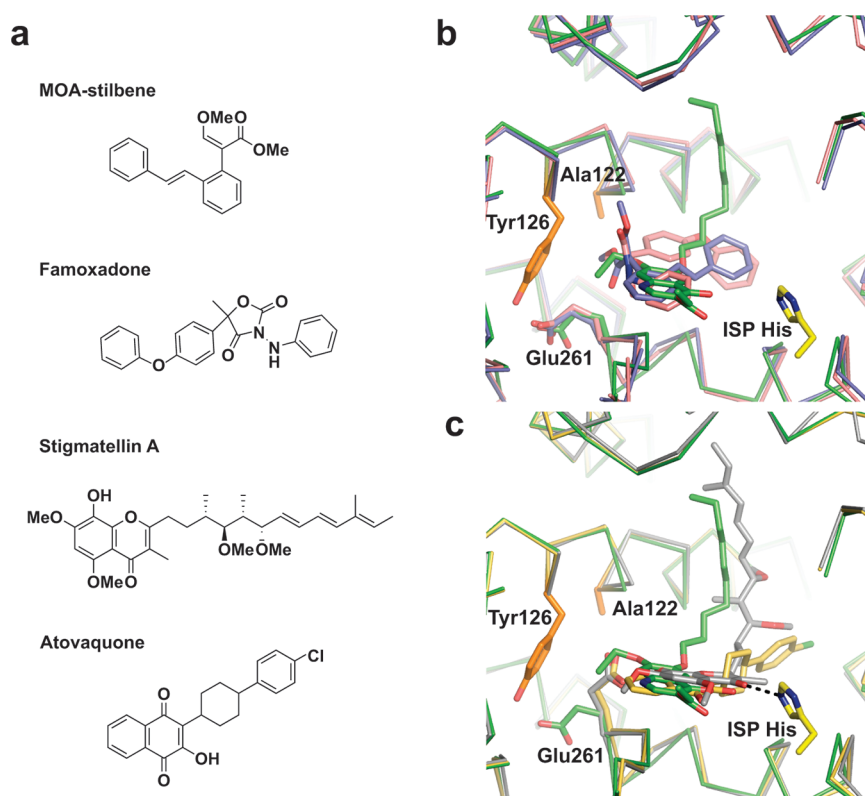


**Figure 3.** Decoquinatone is predicted to be a class Ia inhibitor of the  $Q_o$  site in cytochrome *b*. (a) The chemical structures of putative  $Q_o$  site inhibitors are shown. (b) The docking results between decoquinatone (green) and the *P. falciparum* cytochrome *b* homology model were superimposed onto the cytochrome *b* subunit of bovine cytochrome  $bc_1$  complex co-crystallized with class Ia inhibitors MOAS (slate blue; PDB ID = 1SQQ) and famoxadone (pink; PDB ID = 1L0L) with a rmsd of 0.389 and 0.355 Å, respectively. The resistance-conferring mutations at residues Ala122 and Tyr126 (orange) are shown in the homology model (green). The histidine from the neighboring Rieske ISP subunit is labeled and shown in yellow. The noncarbon atoms are displayed with conventional colors: oxygen in red and nitrogen in blue. (c) Superposition of the decoquinatone and atovaquone (yellow) energy minimization results with the cytochrome *b* subunit of bovine cytochrome  $bc_1$  complex co-crystallized with the class Ib inhibitor stigmatellin A (gray; PDB ID = 1SQX). The rmsd between models is 0.219 Å. The hydrogen bond between stigmatellin A and the histidine residue from the Rieske ISP subunit is depicted as a dashed line. The figure was generated using Pymol software.

Another interesting feature of our study is that two relatively different pharmacophores appear to be acting against the same critical malaria target. These data indicate that predicting the target of a small molecule based on conserved chemical features (e.g., framework analysis<sup>9</sup>) may not be straightforward and that additional experimentation is critical to establish a chemical genetic link between inhibitor and target. Evolution to resistance in combination with genome scanning is a very powerful method in this respect. In general, there is substantially less ambiguity, which is exemplified here as we found only three potential candidate genes. In contrast, affinity chromatography and subsequent mass spectrometry analysis may reveal scores of candidate targets. Furthermore, a cheminformatic analysis may indicate a compound to be a kinase inhibitor but not reveal which one. Of course, here as with other studies we found more than one candidate gene, including protein kinase 4, a plausible target of unknown function. If the body of evidence was not overwhelmingly in favor of cytochrome  $bc_1$  being the target, additional rounds of evolution and genome scanning could reduce ambiguity. This has proven helpful in other cases.<sup>16,18</sup> Thus, although time-consuming, we feel it will be the most attractive way to identify the targets of the thousands of antimalarial compounds identified in recent cell-based screening campaigns.<sup>7–10</sup>

## METHODS

Additional details and sections are available in Supporting Information.

**SYBR Green Proliferation Assay.** 3D7 and other strains of *P. falciparum* were cultured, screened, and used in dose-response assays according to Plouffe *et al.*<sup>7</sup>

**Resistance Selection of Mutagenized Parasites.** A newly established culture of a clonal line of 3D7 (5% parasitemia and 2.5% hematocrit) was placed 15 cm below the UV lamp installed in a biosafety cabinet and UV-irradiated for about 1 min. Once the parasites regained a normal growth profile as checked by blood smear, drug was added to the medium. A starting concentration of half the  $IC_{50}$  value was used and incrementally increased over a 2-month period. Limiting dilution was performed to select a clonal line.

**Single-Step Selection of Atovaquone-Resistant Parasites.** Triplicate cultures of 3D7 parasites were treated with a single concentration of atovaquone (2, 20 or 50 nM) and maintained under drug pressure until parasites could be detected by thin-blood smear.

**Genome Scanning.** Microarray analysis was completed using the methods detailed by Dharia *et al.*<sup>15</sup>

**Sporozoite Invasion Assay and EEF Immunofluorescence Quantification.** An *in vitro* liver stage assay with *P. yoelii* sporozoites was adapted into a high content imaging screen (in press; S. Meister, D. Plouffe, and G. Bonamy) based on the system established by Yalaoui *et al.*<sup>27</sup>



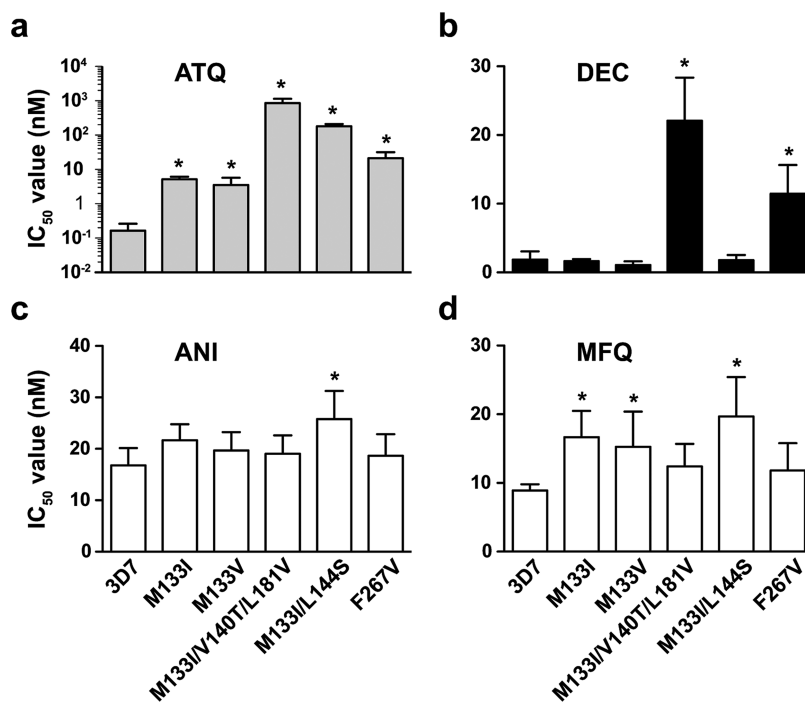


**Figure 4.** A panel of atovaquone-resistant *P. falciparum* lines demonstrate limited cross-resistance to decoquinolate. The IC<sub>50</sub> values against (a) atovaquone (ATQ), (b) decoquinolate (DEC), (c) anisomycin (ANI), and (d) mefloquine (MFQ) are shown for the parental 3D7 strain and five ATQ-R lines. The amino acid substitutions acquired in cytochrome *b* for each resistant line are indicated in the x-axis of the bottom graphs and are denoted by the single-letter amino acid code and amino acid residue number. Statistically significant differences between IC<sub>50</sub> values of the parental 3D7 line and the ATQ-resistant lines were calculated by a two-tailed unpaired *t* test: \**P* < 0.001. IC<sub>50</sub> values for individual ATQ-R lines and the atovaquone-sensitive parental line are represented as means ± SD of three independent experiments performed in quadruplicate.

**Prophylaxis Activity test.** Each ICR female mouse (7 weeks, 26–36 g) was injected with 50,000 *P. yoelii* (17XNL strain) sporozoites *via* the tail vein and immediately dosed by oral gavage with atovaquone (2.5 mg kg<sup>-1</sup>) or decoquinolate (50 mg kg<sup>-1</sup>). Parasitemia was monitored daily by Giemsa staining using blood collected by tail snip. Mice were euthanized when parasitemia exceeded 20%.

**Assaying for Electron Transport Chain Inhibitors.** Generation of the ScDHOD-D10attB line is described by Ke *et al.*,<sup>44</sup> and the SYBR Green proliferation assay was used to determine the IC<sub>50</sub> values of small molecule inhibitors.

**Molecular Modeling.** The *P. falciparum* cytochrome *b* model was built by homology using the X-ray crystallographic coordinates for the bovine cytochrome *bc*<sub>1</sub> complex co-crystallized with stigmatellin A (PDB ID 1PP9) as a template, and fully flexible ligand docking was performed with Glide (version 5.5; Schrödinger).<sup>45</sup> The PyMOL Molecular Graphics System (version 1.2r2, Schrödinger) was used to render the models and prepare figures.

## ASSOCIATED CONTENT

**Supporting Information.** This material is available free of charge *via* the Internet at <http://pubs.acs.org>.

## AUTHOR INFORMATION

### Corresponding Author

\*E-mail: [schultz@scripps.edu](mailto:schultz@scripps.edu); [winzeler@scripps.edu](mailto:winzeler@scripps.edu).

### Present Addresses

<sup>†</sup>Gyeonggi Bio-Center, Suwon, Gyeonggi-do, 443-270, Korea/ College of Pharmacy, Hanyang University, Ansan, Gyeonggi-do, 426-791, Korea.

## Author Contributions

<sup>#</sup>These authors contributed equally to this work.

## ACKNOWLEDGMENT

We extend our gratitude to A. Chatterjee for assistance in triage of the screening data, the snapshot PK team at GNF, and K. Gagaring for technical assistance. This work was supported by a grant from the Medicines for Malaria Venture and a translational research grant (WT078285) from the Wellcome Trust to the Novartis Institute for Tropical Diseases and the Genomics Institute of the Novartis Research Foundation. E.A.W. is supported by the Keck Foundation and by National Institutes of Health grant R01AI090141. A.B.V. is supported by grant R01AI028398 from NIH. This work was supported by the Skaggs Institute for Chemical Biology.

## REFERENCES

- (1) WHO (2010) World Malaria Report 2010, In [http://www.who.int/malaria/world\\_malaria\\_report\\_2010/en/index.html](http://www.who.int/malaria/world_malaria_report_2010/en/index.html).
- (2) Kar, S., and Kar, S. (2010) Control of malaria. *Nat. Rev. Drug Discovery* 9, 511–512.
- (3) McNamara, C., and Winzeler, E. A. (2011) Target identification and validation of novel antimalarials. *Future Microbiol.* 6, 693–704.
- (4) Dasgupta, T., Chitnumsub, P., Kamchonwongpaisan, S., Maneeruttanarungroj, C., Nichols, S. E., Lyons, T. M., Tirado-Rives, J., Jorgensen, W. L., Yuthavong, Y., and Anderson, K. S. (2009) Exploiting structural analysis, in silico screening, and serendipity to identify novel inhibitors of drug-resistant falciparum malaria. *ACS Chem. Biol.* 4, 29–40.
- (5) Kortagere, S., Welsh, W. J., Morrissey, J. M., Daly, T., Ejigiri, I., Sinnis, P., Vaidya, A. B., and Bergman, L. W. (2010) Structure-based

design of novel small-molecule inhibitors of *Plasmodium falciparum*. *J. Chem. Inf. Model.* 50, 840–849.

(6) Yu, M., Kumar, T. R., Nkrumah, L. J., Coppi, A., Retzlaff, S., Li, C. D., Kelly, B. J., Moura, P. A., Lakshmanan, V., Freundlich, J. S., Valderramos, J. C., Vilcheze, C., Siedner, M., Tsai, J. H., Falkard, B., Sidhu, A. B., Purcell, L. A., Gratraud, P., Kremer, L., Waters, A. P., Schiehsler, G., Jacobus, D. P., Janse, C. J., Ager, A., Jacobs, W. R., Jr., Sacchetti, J. C., Heussler, V., Sinnis, P., and Fidock, D. A. (2008) The fatty acid biosynthesis enzyme FabI plays a key role in the development of liver-stage malarial parasites. *Cell Host Microbe* 4, 567–578.

(7) Plouffe, D., Brinker, A., McNamara, C., Henson, K., Kato, N., Kuhlen, K., Nagle, A., Adrian, F., Matzen, J. T., Anderson, P., Nam, T. G., Gray, N. S., Chatterjee, A., Janes, J., Yan, S. F., Trager, R., Caldwell, J. S., Schultz, P. G., Zhou, Y., and Winzeler, E. A. (2008) In silico activity profiling reveals the mechanism of action of antimalarials discovered in a high-throughput screen. *Proc. Natl. Acad. Sci. U.S.A.* 105, 9059–9064.

(8) Guigumede, W. A., Shelat, A. A., Bouck, D., Duffy, S., Crowther, G. J., Davis, P. H., Smithson, D. C., Connelly, M., Clark, J., Zhu, F., Jimenez-Diaz, M. B., Martinez, M. S., Wilson, E. B., Tripathi, A. K., Gut, J., Sharlow, E. R., Bathurst, I., El Mazouni, F., Fowble, J. W., Forquer, I., McGinley, P. L., Castro, S., Angulo-Barturen, L., Ferrer, S., Rosenthal, P. J., Derisi, J. L., Sullivan, D. J., Lazo, J. S., Roos, D. S., Riscoe, M. K., Phillips, M. A., Rathod, P. K., Van Voorhis, W. C., Avery, V. M., and Guy, R. K. (2010) Chemical genetics of *Plasmodium falciparum*. *Nature* 465, 311–315.

(9) Gamo, F.-J., Sanz, L. M., Vidal, J., de Cozar, C., Alvarez, E., Lavandera, J.-L., Vanderwall, D. E., Green, D. V. S., Kumar, V., Hasan, S., Brown, J. R., Peishoff, C. E., Cardon, L. R., and Garcia-Bustos, J. F. (2010) Thousands of chemical starting points for antimalarial lead identification. *Nature* 465, 305–310.

(10) Lucumi, E., Darling, C., Jo, H., Napper, A. D., Chandramohanadas, R., Fisher, N., Shone, A. E., Jing, H., Ward, S. A., Biagini, G. A., DeGrado, W. F., Diamond, S. L., and Greenbaum, D. C. (2010) Discovery of potent small-molecule inhibitors of multidrug-resistant *Plasmodium falciparum* using a novel miniaturized high-throughput luciferase-based assay. *Antimicrob. Agents Chemother.* 54, 3597–3604.

(11) Seman, D. H., Catherman, D. R., Matsui, T., Hayek, M. G., Batson, D. B., Cantor, A. H., Tucker, R. E., Muntifering, R. B., Westendorf, M. L., and Mitchell, G. E., Jr. (1989) Metabolism of decoquinone in chickens and Japanese quail. *Poult. Sci.* 68, 670–675.

(12) Yeates, C. L., Batchelor, J. F., Capon, E. C., Cheesman, N. J., Fry, M., Hudson, A. T., Pudney, M., Trimming, H., Woolven, J., Bueno, J. M., Chicharro, J., Fernandez, E., Fiandor, J. M., Gargallo-Viola, D., Gomez de las Heras, F., Herreros, E., and Leon, M. L. (2008) Synthesis and structure-activity relationships of 4-pyridones as potential antimalarials. *J. Med. Chem.* 51, 2845–2852.

(13) Rathod, P. K., Khosla, M., Gassiss, S., Young, R. D., and Lutz, C. (1994) Selection and characterization of 5-fluoroorotate-resistant *Plasmodium falciparum*. *Antimicrob. Agents Chemother.* 38, 2871–2876.

(14) Rathod, P. K., McErlean, T., and Lee, P.-C. (1997) Variations in frequencies of drug resistance in *Plasmodium falciparum*. *Proc. Natl. Acad. Sci. U.S.A.* 94, 9389–9393.

(15) Dharia, N., Sidhu, A., Cassera, M., Westenberger, S., Bopp, S., Eastman, R., Plouffe, D., Batalov, S., Park, D., Volkman, S., Wirth, D., Zhou, Y., Fidock, D., and Winzeler, E. (2009) Use of high-density tiling microarrays to identify mutations globally and elucidate mechanisms of drug resistance in *Plasmodium falciparum*. *Genome Biol.* 10, R21.

(16) Rottmann, M., McNamara, C., Yeung, B. K., Lee, M. C., Zou, B., Russell, B., Seitz, P., Plouffe, D. M., Dharia, N. V., Tan, J., Cohen, S. B., Spencer, K. R., Gonzalez-Paez, G. E., Lakshminarayana, S. B., Goh, A., Suwanarusk, R., Jegla, T., Schmitt, E. K., Beck, H. P., Brun, R., Nosten, F., Renia, L., Dartois, V., Keller, T. H., Fidock, D. A., Winzeler, E. A., and Diagana, T. T. (2010) Spiroindolones, a potent compound class for the treatment of malaria. *Science* 329, 1175–1180.

(17) Dharia, N. V., Plouffe, D., Bopp, S. E., Gonzalez-Paez, G. E., Lucas, C., Salas, C., Soberon, V., Bursulaya, B., Kochel, T. J., Bacon, D. J., and Winzeler, E. A. (2010) Genome scanning of Amazonian *Plasmodium*

*falciparum* shows subtelomeric instability and clindamycin-resistant parasites. *Genome Res.* 20, 1534–1544.

(18) Istvan, E. S., Dharia, N. V., Bopp, S. E., Gluzman, I., Winzeler, E. A., and Goldberg, D. E. (2011) Validation of isoleucine utilization targets in *Plasmodium falciparum*. *Proc. Natl. Acad. Sci. U.S.A.* 108, 1627–1632.

(19) Fry, M., and Williams, R. B. (1984) Effects of decoquinone and clodipol on electron transport in mitochondria of *Eimeria tenella* (Apicomplexa: Coccidia). *Biochem. Pharmacol.* 33, 229–240.

(20) McFadden, D. C., and Boothroyd, J. C. (1999) Cytochrome b mutation identified in a decoquinone-resistant mutant of *Toxoplasma gondii*. *J. Eukaryotic Microbiol.* 46, 81S–82S.

(21) Fry, M., and Pudney, M. (1992) Site of action of the antimalarial hydroxynaphthoquinone, 2-[trans-4-(4'-chlorophenyl) cyclohexyl]-3-hydroxy-1,4-naphthoquinone (566C80). *Biochem. Pharmacol.* 43, 1545–1553.

(22) Painter, H. J., Morrissey, J. M., Mather, M. W., and Vaidya, A. B. (2007) Specific role of mitochondrial electron transport in blood-stage *Plasmodium falciparum*. *Nature* 446, 88–91.

(23) Korsinczky, M., Chen, N., Kotecka, B., Saul, A., Rieckmann, K., and Cheng, Q. (2000) Mutations in *Plasmodium falciparum* cytochrome b that are associated with atovaquone resistance are located at a putative drug-binding site. *Antimicrob. Agents Chemother.* 44, 2100–2108.

(24) Mather, M. W., Darrouzet, E., Valkova-Valchanova, M., Cooley, J. W., McIntosh, M. T., Daldal, F., and Vaidya, A. B. (2005) Uncovering the molecular mode of action of the antimalarial drug atovaquone using a bacterial system. *J. Biol. Chem.* 280, 27458–27465.

(25) Davies, C. S., Pudney, M., Nicholas, J. C., and Sinden, R. E. (1993) The novel hydroxynaphthoquinone 566C80 inhibits the development of liver stages of *Plasmodium berghei* cultured in vitro. *Parasitology* 106 (Pt 1), 1–6.

(26) Mahmoudi, N., Ciceron, L., Franetich, J. F., Farhati, K., Silvie, O., Eling, W., Sauerwein, R., Danis, M., Mazier, D., and Derouin, F. (2003) In vitro activities of 25 quinolones and fluoroquinolones against liver and blood stage *Plasmodium* spp. *Antimicrob. Agents Chemother.* 47, 2636–2639.

(27) Yalaoui, S., Zougbede, S., Charrin, S., Silvie, O., Arduise, C., Farhati, K., Boucheix, C., Mazier, D., Rubinstein, E., and Froissard, P. (2008) Hepatocyte permissiveness to *Plasmodium* infection is conveyed by a short and structurally conserved region of the CD81 large extracellular domain. *PLoS Pathog.* 4, e1000010.

(28) Gutteridge, W. E., Dave, D., and Richards, W. H. (1979) Conversion of dihydroorotate to orotate in parasitic protozoa. *Biochim. Biophys. Acta* 582, 390–401.

(29) Hines, V., and Johnston, M. (1989) Analysis of the kinetic mechanism of the bovine liver mitochondrial dihydroorotate dehydrogenase. *Biochemistry* 28, 1222–1226.

(30) Gojković, Z., Knecht, W., Zameitat, E., Warneboldt, J., Coutelis, J. B., Pynyaha, Y., Neuveglise, C., Møller, K., Löffler, M., and Piškur, J. (2004) Horizontal gene transfer promoted evolution of the ability to propagate under anaerobic conditions in yeasts. *Mol. Genet. Genomics* 271, 387–393.

(31) Crofts, A. R., Barquera, B., Gennis, R. B., Kuras, R., Guergova-Kuras, M., and Berry, E. A. (1999) Mechanism of ubiquinol oxidation by the bc(1) complex: different domains of the quinol binding pocket and their role in the mechanism and binding of inhibitors. *Biochemistry* 38, 15807–15826.

(32) Link, T. A., Haase, U., Brandt, U., and von Jagow, G. (1993) What information do inhibitors provide about the structure of the hydroquinone oxidation site of ubiquinol: cytochrome c oxidoreductase? *J. Bioenerg. Biomembr.* 25, 221–232.

(33) Esser, L., Quinn, B., Li, Y. F., Zhang, M., Elberry, M., Yu, L., Yu, C. A., and Xia, D. (2004) Crystallographic studies of quinol oxidation site inhibitors: a modified classification of inhibitors for the cytochrome bc(1) complex. *J. Mol. Biol.* 341, 281–302.

(34) Gao, X., Wen, X., Yu, C., Esser, L., Tsao, S., Quinn, B., Zhang, L., Yu, L., and Xia, D. (2002) The crystal structure of mitochondrial cytochrome bc1 in complex with famoxadone: the role of aromatic-aromatic interaction in inhibition. *Biochemistry* 41, 11692–11702.



(35) Kessl, J. J., Meshnick, S. R., and Trumppower, B. L. (2007) Modeling the molecular basis of atovaquone resistance in parasites and pathogenic fungi. *Trends Parasitol.* 23, 494–501.

(36) Barton, V., Fisher, N., Biagini, G. A., Ward, S. A., and O'Neill, P. M. (2010) Inhibiting Plasmodium cytochrome bc1: a complex issue. *Curr. Opin. Chem. Biol.* 14, 440–446.

(37) Schwobel, B., Alifrangis, M., Salanti, A., and Jelinek, T. (2003) Different mutation patterns of atovaquone resistance to *Plasmodium falciparum* in vitro and in vivo: rapid detection of codon 268 polymorphisms in the cytochrome b as potential in vivo resistance marker. *Malaria J.* 2, 5.

(38) Ekala, M.-T., Khim, N., Legrand, E., Randrianarivojosia, M., Jambou, R., Fandeur, T., Menard, D., Assi, S.-B., Henry, M.-C., Rogier, C., Bouchier, C., and Mercereau-Puijalon, O. (2007) Sequence analysis of *Plasmodium falciparum* cytochrome b in multiple geographic sites. *Malaria J.* 6, 164.

(39) Happi, C. T., Gbotosho, G. O., Folarin, O. A., Milner, D., Sarr, O., Sowunmi, A., Kyle, D. E., Milhous, W. K., Wirth, D. F., and Oduola, A. M. (2006) Confirmation of emergence of mutations associated with atovaquone-proguanil resistance in unexposed *Plasmodium falciparum* isolates from Africa. *Malaria J.* 5, 82.

(40) Peters, J. M., Chen, N., Gatton, M., Korsinczky, M., Fowler, E. V., Manzetti, S., Saul, A., and Cheng, Q. (2002) Mutations in cytochrome b resulting in atovaquone resistance are associated with loss of fitness in *Plasmodium falciparum*. *Antimicrob. Agents Chemother.* 46, 2435–2441.

(41) Japrun, D., Leartsakulpanich, U., Chusacultanachai, S., and Yuthavong, Y. (2007) Conflicting requirements of *Plasmodium falciparum* dihydrofolate reductase mutations conferring resistance to pyrimethamine-WR99210 combination. *Antimicrob. Agents Chemother.* 51, 4356–4360.

(42) Cross, R. M., Monastyrskiy, A., Mutka, T. S., Burrows, J. N., Kyle, D. E., and Manetsch, R. (2010) Endochin optimization: structure-activity and structure-property relationship studies of 3-substituted 2-methyl-4(1H)-quinolones with antimalarial activity. *J. Med. Chem.* 53, 7076–7094.

(43) Winter, R., Kelly, J. X., Smilkstein, M. J., Hinrichs, D., Koop, D. R., and Riscoe, M. K. (2010) Optimization of endochin-like quinolones for antimalarial activity. *Exp. Parasitol.* 127, 545–551.

(44) Ke, H., Morrisey, J. M., Ganesan, S. M., Painter, H. J., Mather, M. W., and Vaidya, A. B. (2011) Variation among *Plasmodium falciparum* strains in their reliance on mitochondrial electron transport chain function. *Eukaryot. Cell* 10, 1053–1061.

(45) Halgren, T. A., Murphy, R. B., Friesner, R. A., Beard, H. S., Frye, L. L., Pollard, W. T., and Banks, J. L. (2004) Glide: a new approach for rapid, accurate docking and scoring. 2. Enrichment factors in database screening. *J. Med. Chem.* 47, 1750–1759.